

# Dielectric response of magnetite nanoparticles

Balakrishnan Chinnu<sup>a</sup>, K. R. S. Prasad<sup>a</sup>, G. Narsinga Rao<sup>b</sup>, K. Suresh Babu<sup>b\*</sup>

<sup>a</sup>Department of Chemistry, Koneru Lakshmaiah Education Foundation, Vaddeswaram, Guntur,  
Andhra Pradesh, 522502, India.

<sup>b</sup>Department of Freshmen Engineering, Marri Laxman Reddy Institute of Technology and  
Management, Hyderabad, Telangana, 500 043, India.

## **Abstract:**

*The dielectric properties of magnetite nanoparticles for different grain sizes with different test frequency  $f$  and at different temperature  $T$  were investigated. In magnetite nanoparticles the dielectric relaxation follows thermally activated process. The activation energy is obtained around 98 meV for 15 nm particles of magnetite. The observed activation energies varies with decreasing particle size. The observation of a sudden drop in the field-cooled dc magnetic susceptibility  $\chi(T)$  curve at 100 K infers that the slope change in dielectric relaxation is related to the occurrence of the Verwey transition in the nanoparticles. It is also shows superparamagnetism which useful for Hyperthermia as well as Magnetic Resonance imaging in Medical Parameters.*

**Keywords:** Magnetite nanoparticles; dielectric relaxation; activation energy; thermally activated process; Verwey transition.

## **Introduction:**

Magnetite ( $\text{Fe}_3\text{O}_4$ ) has attracted intensive attention because it's intriguing properties as well as the potential applications in spin-electronics. It also displays a rather unique electronic phase transition is the Verwey transition at  $T_v \sim 120$  K [1], whose explanation has remained a challenge to modern condensed matter physics [2,3]. The Verwey transition has been observed mainly in single crystals or large grain polycrystalline samples with a composition very close to that of magnetite. Recently, the Verwey transition was found in nanocrystalline magnetite thin films [4] and nanometric powders [5] using magnetic susceptibility measurements, but without the accompanying conductivity changes. Some other reports the transition did not appear in magnetic measurements, while a change in tunneling transport measurements [6].

For a stoichiometric magnetite, the first order magnetocrystalline anisotropy constant changes sign on passing through an isotropic point ( $T_k$ ) at  $\sim 130$  K [7]. A few degrees below  $T_k$  the crystal structure changes from cubic to monoclinic at  $T_v$  [8]. The large increase in the magnetocrystalline anisotropy is a result of a sharp reduction in the mobility of electrons from 3d shells which move or

'hop' between the  $\text{Fe}^{3+}$  and  $\text{Fe}^{2+}$  cations on the  $B$ -sublattice, on cooling through  $T_v$  [7,8]. Mott's view of the Verwey transition, as corresponding to the phase changing of a Wigner glass ( $T > T_v$ ) into a Wigner crystal ( $T < T_v$ ), describes most adequately the various low temperature mechanisms in  $\text{Fe}_3\text{O}_4$  in terms of tunneling and variable range hopping of small polarons. The materials in which hopping conduction dominates the electrical transport, dielectric measurements provide important information because of hopping process has a high probability of involving a dielectric relaxation [9-12]. In spite of the vast amount work done on  $\text{Fe}_3\text{O}_4$  in the form of bulk as well as nanoparticles by a variety of techniques, there has been scarce of report on temperature and frequency dependent dielectric measurements on magnetite nanoparticle to date. In this paper, the dielectric properties of magnetite nanoparticles for different grain sizes and bulk with test frequency  $f$  in the range from 20 Hz to 1 MHz and at temperature  $T$  between 10 K and 300 K were investigated

### Experimental

The  $\text{Fe}_3\text{O}_4$  nanoparticles were prepared using co-precipitation method under inert atmosphere.  $\text{Fe}_3\text{O}_4$  nanoparticles size were depends on pH value of co-precipitation method [13,14]. The source of iron solution was prepared by dissolving 2:1 ratio of  $\text{FeCl}_3 \cdot 6\text{H}_2\text{O}$  and  $\text{FeCl}_2 \cdot 4\text{H}_2\text{O}$  in deoxygenated water. The NaOH (1 M) solution is added into the iron source under the protection of  $\text{N}_2$  gas, a various pH value of and 12 were obtained. The black precipitate was formed which is isolated with magnetic field, and the supernatant was removed. These precipitates were washed several times, to neutralize the anionic charges with dilute acid (0.01 M HCl) was added. The structural characterization of the as prepared  $\text{Fe}_3\text{O}_4$  nanoparticles was checked by room temperature powder X-ray diffraction (XRD). Using the transmission electron microscope (TEM), the size, shape and morphology of particles were measured.

The capacitance ( $C$ ) and dielectric loss tangent ( $\tan \delta$ ) were carried out in the wide frequency range between 80 K and 300 K. The measurements were performed on the circular dish-shaped (6 mm diameter and 1 mm thickness) samples with silver paint coated on two sides as the electrodes. The field cooled (FC) and zero field cooled (ZFC) magnetization curves were measured in a commercial SQUID magnetometer with the temperature range from 4 K to 300 K in an applied field of 10 mT.

### Results and discussion

Figure 1 shows the temperature dependence of  $\epsilon'$  for 15 nm size magnetite nanoparticles with various test frequencies. The  $\epsilon'(T)$  curves for these nanoparticles exhibits quite different behavior than that of the bulk magnetite. For  $T < 100$  K,  $\epsilon'(T)$  displays a rapid decrease with decreasing temperature to a value as low as 10 with independent of temperature and frequency. The rapid decrease in  $\epsilon'(T)$  corresponds to peak in the  $\tan\delta$ . Figure 2 shows the temperature dependence of

$\tan\delta$  for 15 nm size magnetite nanoparticles with various test frequencies. The peak position of  $\tan\delta$  shifts to higher temperature as the measuring frequency increases (Fig. 2), indicating thermally activated relaxation process. The dielectric relaxation of these nanoparticles were appear at higher temperature (85 K to 130 K) compare to that of the bulk magnetite. The  $f_{\max}$  versus inverse temperature ( $1/T_p$ ) was depicted in Fig. 3. The fitting results agree with the Arrhenius law ( $f = f_0 \exp(E_a/k_B T_p)$ ) with two linear regions at higher and lower temperatures, respectively, with the intersection temperature  $T \sim 100$  K. The activation energy for the high temperature region is 98.11 meV and 55.1 meV for low temperature region. Both activation energies and intersection temperature varies with decreasing particle size.

In order to verify the nature of the relaxations, the dc conductivity extracted from the experimentally observed ac conductivity at several temperatures, as shown in Fig. 4. The slowly varying region at the high frequency shows a power law behavior. With increasing  $T$ , the power law region shifts to higher value of  $f$  and for  $T > 100$  K, it goes out of the measurable frequency range (1 MHz) of our experiment. Such power law region can be fitted with an empirical universal response (UDR) formula [15]

$$\sigma = \sigma_{dc} + \sigma_0 f^s \quad (4)$$

where  $\sigma_{dc}$  is the bulk conductivity,  $\sigma_0$  is a UDR constant,  $f$  is the frequency, and  $s$  is an exponent smaller than 1. Fitting this equation to the high frequency region of the data yielded  $\sigma_{dc}$ ,  $\sigma_0$ , and  $s$  at different temperatures. The temperature dependence of  $\sigma_{dc}$  thus obtained was analyzed by fitting the data to the Arrhenius relation. These results are depicted in Fig. 5, the best fit values of  $\sigma_0$  and  $E_a$  for magnetite nanoparticles are  $3.159 \times 10^{-4}$  S/m and 46.7 meV. Both dielectric relaxation and conductivity follow the thermally activated process with similar value of the activation energy. This indicates the close correlation between the electric conduction and the dielectric polarization below 100 K.

The modulus formalism ( $M^* = M' + iM''$ ) has the advantage of eliminating the contact contributions [16,17]. The plots of  $M'$  vs  $M''$  at different temperatures  $T$  are shown in Fig. 6 for nano magnetite samples. For  $T \geq 200$  K, the single semicircle arc corresponding to grain boundary components are observed in nano magnetite (Fig. 6). As the temperature decreased to  $\sim 100$  K, two semicircle arcs are entered within the measured frequency range for both the samples. The above results reveal that at  $T > 100$  K grain boundary effects are dominating, whereas below 100 K contributions of intrinsic grains in the present sample.

The temperature dependence of field cooled (FC) and zero field cooled (ZFC) magnetization curves of 15 nm size particles are showed in Fig. 7. FC and ZFC curves coincide at high temperature

and they begin to separate as the temperature decreases and the ZFC curve exhibit maxima. Such behavior is characteristic of superparamagnetism [18-20] and is due to the progressive deblocking of particles of increasing size as the temperature rises. For further decreasing temperature ZFC curve shows relatively fast decreasing rate below 100 K and FC curve clearly exhibits a small drop at about 100 K (inset Fig. 8) which is a characteristic of Verwey transition ( $T_v$ ). The absence of sharp drop in ZFC curve below Verwey transition is probably due to the larger magnetization effects arising from the superparamagnetic nature of the particles. The observed transition indicates that the charge ordering between  $Fe^{2+}$  and  $Fe^{3+}$  on the octahedral sites exists in  $Fe_3O_4$  nanoparticles at temperature lower than 100 K. This result infers that such change of linearity in dielectric relaxation is related to the occurrence of the Verwey transition in the nanoparticles.

### Conclusions

The dielectric response of magnetite nanoparticles were studied in the wide frequency range between 80 K and room temperature. The dielectric relaxation phenomena were found in nano magnetite samples at different temperature ranges. For magnetite the dielectric relaxation follows thermally activated process with two linear regions with the intersection temperature  $T \sim 100$  K. Both activation energies and intersection temperature varies with decreasing particle size. The observation of a sudden drop in the field-cooled dc magnetic susceptibility  $\chi(T)$  curve at 100 K infers that such change of linearity in dielectric relaxation is related to the occurrence of the Verwey transition in the nanoparticles.

### Acknowledgements

The Authors greatly thankful for the support from the management of Koneru Lakshmaiah Education Foundation (KLEF), Principal and Management of Marri Laxman Reddy Institute of Technology and Management (MLRITM) for providing facilities. This work is financially supported by the Department of Science and Technology (DST), Science and Engineering Research Board (SERB), Government of India, New Delhi, No: ECR/2016/001647.

### References:

1. E. J. W. Verwey, Nature (London) **144**, 327 (1939).
2. F. Walz, J. Phys.: Condens. Matter **14**, R 285 (2002)
3. J. Garcia and G. Subias, J. Phys.: Condens. Matter **16**, R 145 (2004)
4. J. Tang, K.-Y. Wang, and W. Zhou, J. Appl. Phys. **89**, 7690 (2001).
5. N. Guigue-Millot, N. Keller, and P. Perriat, Phys. Rev. B **64**, 12402 (2001).
6. P. Poddar, T. Fried and G. Markovich, Phys. Rev. B **65**, 172405 (2002)
7. M. Izumi, T. F. Koetzle, G. Shirane, S. Chikazumi, M. Matsui and S. Todo, Acta Crystallogr.,

- Sect. B: Struct. Sci. **38**, 2121 (1982).
8. A. Mansingh, J. M. Reyes and M. Sayer, *J. Non-Cryst. Solids* **7**, 12 (1972)
  9. R. Gehlig and E. Salje, *Phil. Mag. B* **47**, 229 (1983)
  10. H. A. A. Sidek, I. T. Collier, R. N. Hampton, G. A. Saunders and B. Bridge *Phil. Mag. B* **59**, 221 (1989)
  11. E. Iguchi, N. Kubota, T. Nakamori, N. Yamamoto and K. J. Lee *Phys. Rev. B* **43**, 8646 (1991)
  12. W. H. Jung and E. Iguchi, *Phil. Mag. B* **73**, 873 (1996)
  13. G. Narsinga Rao, Y. D. Yao, Y. L. Chen, K. T. Wu, and J. W. Chen, *Phys. Rev. E* **72**, 031408 (2005)
  14. Ch. Hemalatha, K. Suresh Babu and G. Narsinga Rao, *Green engineering*, 10, (2020)
  15. A. K. Jonscher, *Nature (London)* **267**, 673 (1977).
  16. D. C. Sinclair, T. B. Adams, F. D. Morrison, and A. R. West, *Appl. Phys. Lett.* **89**, 212905 (2002).
  17. L. Chen, C. L. Chen, Y. Lin, Y. B. Chen, X. H. Chen, Bontchev, C. Y. Park, and A. J. Jacobson, *Appl. Phys. Lett.* **82**, 2317 (2003).
  18. L. Neel, *Ann. Geophys.*, **5** (1949) 99
  19. A. H. Morrish, *The Physical Principles of Magnetism*, Wiley, New York, 1965
  20. S. Morup, F. Bodker, P. V. Hendriksen and S. Linderoth, *Phys. Rev. B.* **52** (1995) 287

### Figure Captions

- Fig. 1. The temperature dependence of real permittivity  $\epsilon'$  of nano magnetite with various test frequencies.
- Fig. 2. The temperature dependence of imaginary part of  $\tan\delta$  of nano magnetite with various test frequencies.
- Fig. 3. The measuring frequency  $f$  versus the reciprocal of the peak temperature  $T_p$  obtained from the  $\tan \delta$  curve for nano magnetite. The solid line is fit to the Arrhenius model.
- Fig. 4. The frequency dependence of ac conductivity ( $\sigma_{ac}$ ) at selected temperatures for nano magnetite. The solid line is UDR model fit.
- Fig. 5.  $\sigma_{DC}$  (T) versus  $1/T$  curve for nano magnetite. The solid line is Arrhenius fit.
- Fig. 6. Complex modulus ( $M^*$ ) plot ( $M''$  vs  $M'$ ) at different temperatures for nano magnetite.
- Fig. 7. The temperature dependence of field cooled (FC) and zero field cooled (ZFC) magnetization curves of nano magnetite. Inset is expanded view.

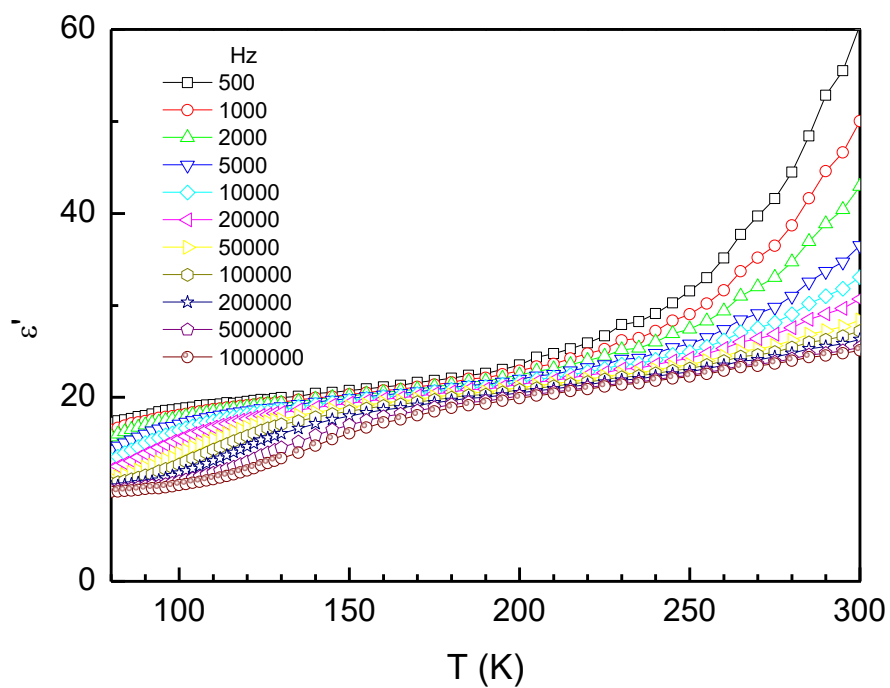


Fig. 1

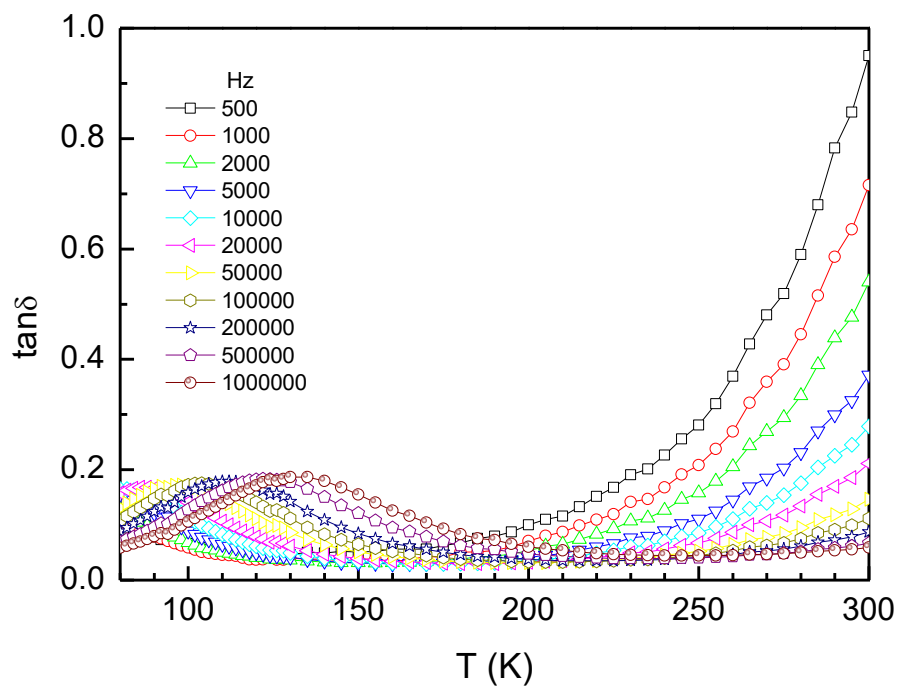


Fig. 2

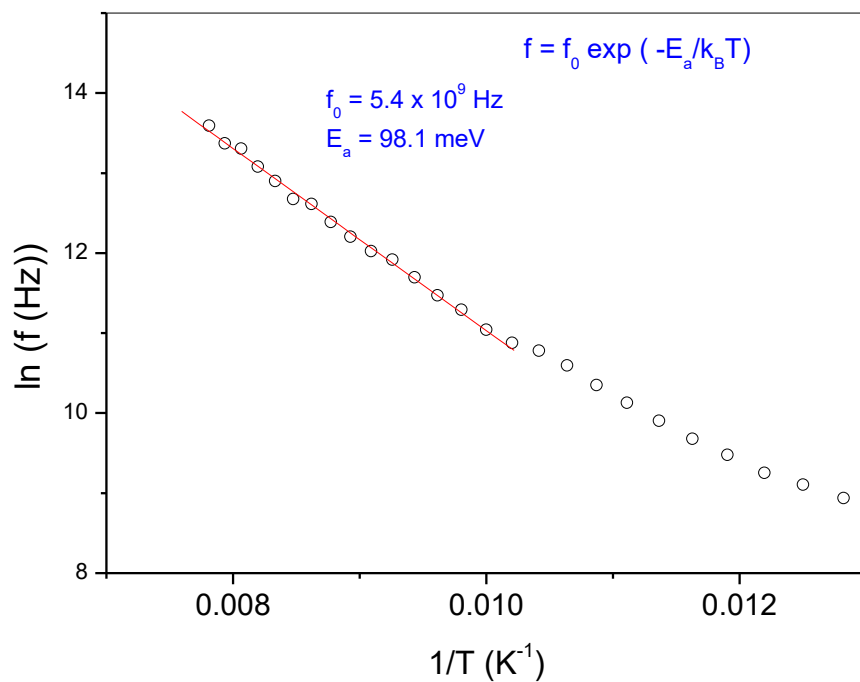


Fig. 3

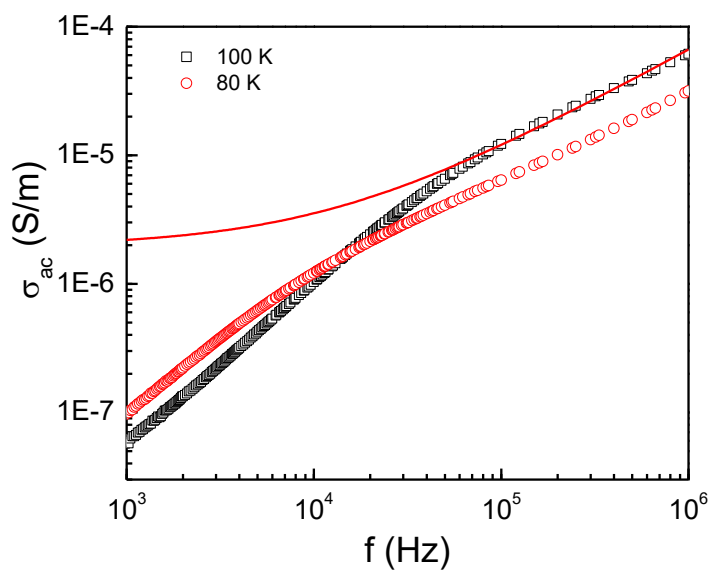


Fig. 4

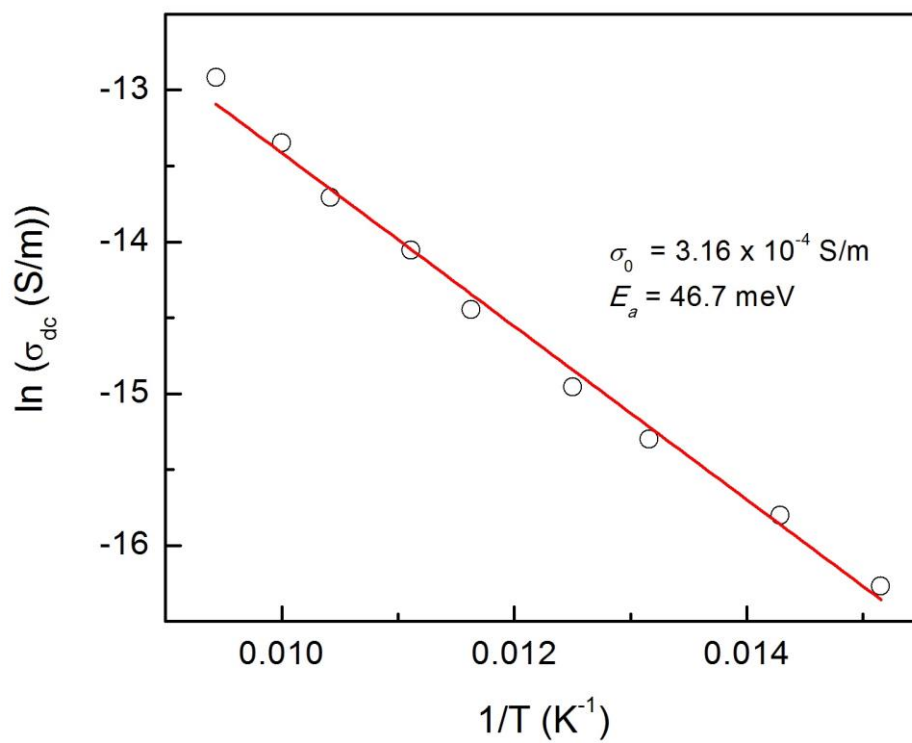


Fig. 5

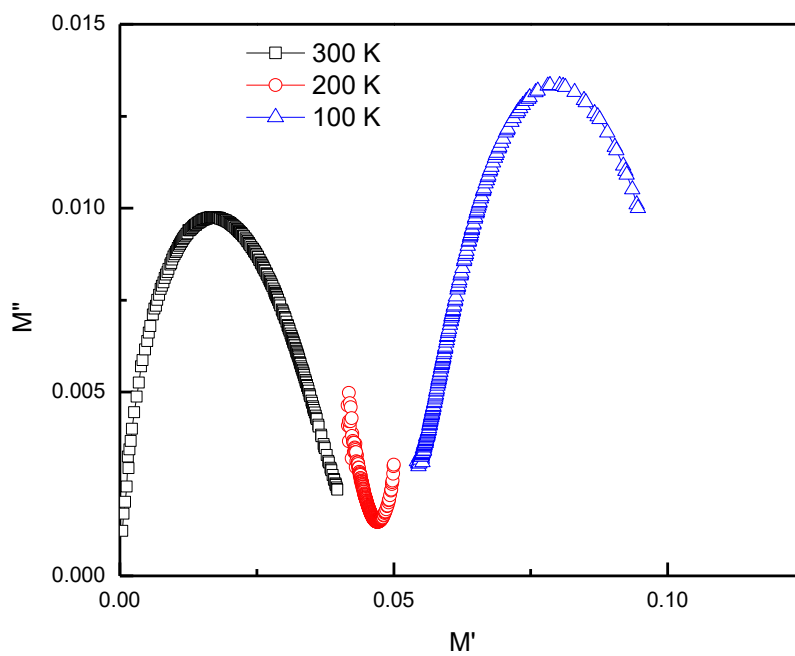


Fig. 6

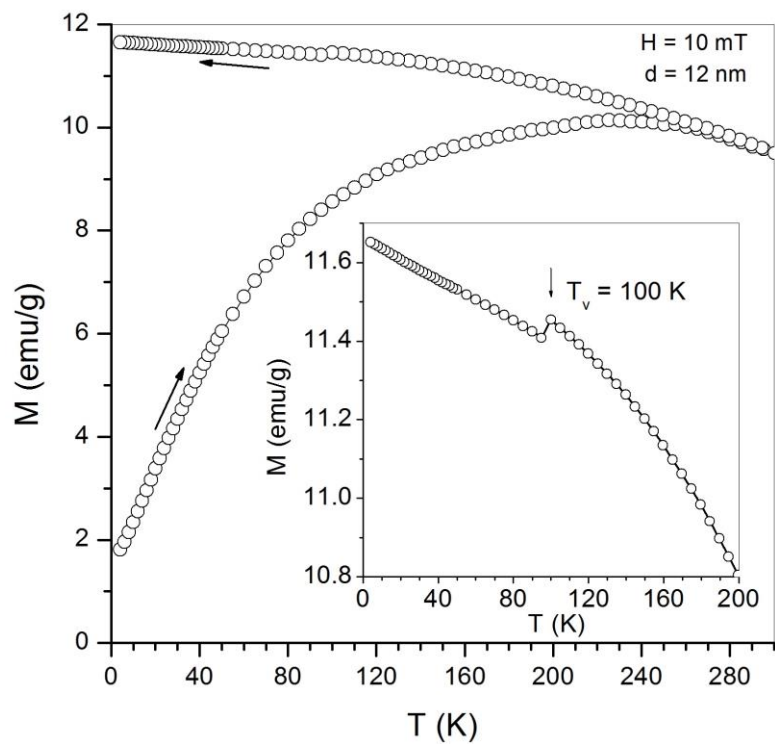


Fig. 7